Mar Biotechnol (2011) 13:751–763
DOI 10.1007/s10126-010-9336-5

ORIGINAL ARTICLE

# Effects of Asian Dust Storms on *Synechococcus* Populations in the Subtropical Kuroshio Current

**Chih-Ching Chung · Jeng Chang · Gwo-Ching Gong · Shih-Chieh Hsu · Kuo-Ping Chiang · Chia-Wen Liao**

Received: 7 May 2010 / Accepted: 4 October 2010 / Published online: 14 December 2010


**Abstract** Asian dust storms (ADSs) are the major source of dust deposition in the Northwest Pacific Ocean. To gain a better understanding on how ADSs affect the ecology of picophytoplankton in this oligotrophic region, five oceanographic cruises were conducted between March 15 and April 15, 2006 on a segment of the Kuroshio Current near the shelf break of the East China Sea (25.05° N, 123.15° E). During the study period, three ADS events were recorded and increases in nutrient concentrations as well as mixing depths were observed. Most of the ADS events stimulated the growth of *Synechococcus*, but the abundance of *Prochlorococcus* either remained unaffected or showed mild declines. A more detailed study was conducted during the ADS event between March 16 and 19. Phylogenetic analysis of 16S ribosomal RNA nucleotide sequences revealed that most of the newly appeared *Synechococcus* belonged to the clade II lineage. Furthermore, messenger RNA (mRNA) levels of three nutrient deficiency indicators, including *idiA* (an iron deficiency indicator), *ntcA* (a nitrogen deficiency indicator), and *pstS* (a phosphorus deficiency indicator), were analyzed by real-time quantitative reverse-transcription polymerase chain reaction. As this ADS event proceeded, mRNA levels of all these indicators decreased from relatively high to non-detectable values. These results suggest that the contributions of iron, nitrogen, and phosphate by the dust deposition from ADSs promote the growth of *Synechococcus* in the Kuroshio Current.

**Keywords** Dust storm · Picophytoplankton · *Synechococcus* · *Prochlorococcus*

C.-C. Chung
Center for Marine Bioenvironment and Biotechnology,
National Taiwan Ocean University,
Keelung 20224 Taiwan, Republic of China

C.-C. Chung (✉) · J. Chang · G.-C. Gong · K.-P. Chiang
Institute of Marine Environmental Chemistry and Ecology,
National Taiwan Ocean University,
Keelung 20224 Taiwan, Republic of China
e-mail: chungcc@mail.ntou.edu.tw

J. Chang · C.-W. Liao
Institute of Marine Biology, National Taiwan Ocean University,
Keelung 20224 Taiwan, Republic of China

S.-C. Hsu
Research Center for Environmental Changes, Academia Sinica,
Nankang,
Taipei 11529 Taiwan, Republic of China

K.-P. Chiang
Department of Environmental Biology and Fishery Science,
National Taiwan Ocean University,
Keelung 20224 Taiwan, Republic of China

## Introduction

The magnitude of atmospheric–upper ocean interactions leads to changes in the carbon dioxide ($CO_2$) uptake ability of phytoplankton (Falkowski et al. 2000). Dust deposition, one of the important atmospheric forcing events, can supply bioavailable nutrients and trace metals for phytoplankton growth in oligotrophic open oceans (Jickells 1995; Goudie and Middleton 2001; Herut et al. 2005; Jickells et al. 2005; Kellogg and Griffin 2006; Hsu et al. 2009). For example, aerosols from the Saharan Desert significantly increase primary production in surface waters of the Mediterranean Sea (Herut et al. 2005). Iron and phosphate supplied by Saharan dust particles enhance nitrogen fixation of *Trichodesmium* in the North Atlantic (Mills et al. 2004). Likewise, Asian dust storms (ADSs), which originate from the Gobi

Desert, result in a near doubling of the phytoplankton carbon biomass in the North Pacific Ocean (Bishop et al. 2002). In addition, strong atmospheric–oceanic disturbances accompanying dust storm events may bring deep nutrients to the sea surface, which further increases primary productivity and particulate organic carbon (POC) export fluxes in the Northwest Pacific Ocean (Yuan and Zhang 2006; Hung et al. 2009).

*Prochlorococcus* and *Synechococcus*, the predominant components in photosynthetic picoplankton (size < 2 μm), are responsible for up to 50% of the $CO_2$ fixation in the open ocean and are speculated to make a notable contribution to carbon export from surface to deep waters (Waterbury et al. 1979; Chisholm et al. 1988; Goericke and Welschmeyer 1993; Liu et al. 1995, 1997; Richardson and Jackson 2007). The global distributions of *Prochlorococcus* and *Synechococcus* are diverse. *Prochlorococcus* occupies ultraoligotrophic environments between 40° N and 40° S. In contrast, *Synechococcus* is ubiquitous in mesotrophic waters, such as inshore and coastal regions (Campbell and Vaulot 1993; Blanchot and Rodier 1996; Partensky et al. 1999a, b; Chiang et al. 2002; Ting et al. 2002; Zwirglmaier et al. 2008). Furthermore, due to their tiny cell sizes and very different physiological characteristics, the distribution and succession of picophytoplankton are easily influenced by abrupt environmental changes. For example, in surface waters of the Eastern Mediterranean Sea, a significant increase in *Synechococcus* abundance with a concomitant disappearance of *Prochlorococcus* was observed during a dust storm event (Herut et al. 2005). Nutrients, heavy metals, and anthropogenic materials carried in atmospheric deposition were considered to be possible factors causing changes in the picophytoplankton assemblages (Herut et al. 2005; Paytan et al. 2009). However, the detailed mechanisms underlying population succession during dust storm periods still need to be investigated.

The relationship between the population dynamics of picophytoplankton and environmental changes is very complex, and application of molecular indicators provides a more direct approach to reveal the response of cells in their natural habitats. Recently, several nutrient deficiency indicators were developed to detect different nutrient stresses in *Synechococcus* and *Prochlorococcus*. Expression of IdiA (an iron deficiency protein A) is a protein responsive to iron starvation in *Synechococcus*, and polyclonal antiserum against IdiA was used to successfully label iron-stressed cells in the field (Webb et al. 2001; Rivers et al. 2009). On the other hand, the *pstS* gene encodes a high-affinity phosphate uptake protein, which was used to reveal that ambient phosphate level was a key factor in the seasonal succession of picophytoplankton in the Red Sea (Fuller et al. 2005). Similarly, the transcription level of a global nitrogen regulator, *ntcA*, was applied to reflect the nitrogen assimilation status in natural populations of *Synechococcus* (Lindell and Post 2001; Lindell et al. 2005).

In the past decade, one part of the integrated program, Long-term Observation and Research of the East China Sea, a Taiwanese contribution to the international program, Surface Ocean-Lower Atmosphere Study, has been conducted to track the influences of ADSs on picophytoplankton ecology in surface waters of the open ocean. As the western boundary current of the North Pacific Ocean, the Kuroshio Current flows northward along the outer margin of the East China Sea (Nitani 1972; Wong et al. 2000). Kuroshio surface waters are ultraoligotrophic in nature with chlorophyll *a* concentrations constantly below 0.2 mg $m^{-3}$ (Gong et al. 1997, 1999), and the predominant group of picoplankton in the Kuroshio Current is *Prochlorococcus* (Jiao et al. 2002; Katano et al. 2007). This "clean" environment is an excellent place to study the effects of ADSs on picophytoplankton ecology. In this study, autotrophic picoplankton were identified and enumerated by flow cytometry. At the same time, a 16S ribosomal RNA (rRNA) phylogenetic analysis was applied to reveal the genetic composition and community dynamics of the cyanobacterial picoplankton. Furthermore, the nutrient utilization status of cyanobacterial picoplankton was revealed by the expression profiles of the nutrient stress-related genes, *idiA*, *ntcA*, and *pstS*. With this information, the influences of dust deposition on the ecology of picophytoplankton in the subtropical Kuroshio Current were comprehensively described. Moreover, rising atmospheric $CO_2$ concentration and resultant temperature increase gradually start to affect global marine ecosystems. It has been documented that artificial iron fertilization can efficiently enhance phytoplankton growth and primary productivity particularly in the high-nitrate low-chlorophyll oceans (Boyd et al. 2007). Similar operations are suggested as promising approaches for $CO_2$ sequestration from the atmosphere to the ocean. However, further questions on how iron enrichment affects the assimilation of other nutrients in phytoplankton need to be simultaneously considered. In this study, our molecular diagnostic method for assessing nutrient utilization in cyanobacterial picoplankton provides a convenient way to clarify these questions in the future.

## Materials and Methods

### Sample Collection

An observation station (ADS station) was established at 25.05° N, 123.15° E, located in the oligotrophic Kuroshio Current near the outer edge of the East China Sea (Fig. 1). Five cruises aboard the research vessel *Ocean Researcher II* (ORII) were conducted during the period from March 15 to

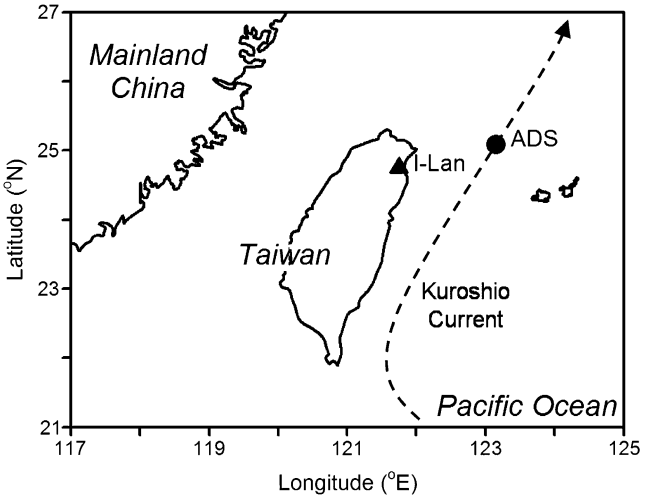


**Fig. 1** Location of the Asian dust storm (ADS) station (*solid circle*, 25.05° N, 123.15° E) in the oligotrophic subtropical Kuroshio Current near the outer edge of the East China Sea. The amount of the dust deposition ($PM_{10}$) was monitored at the Taiwanese Environmental Protection Administration's I-Lan station (*solid triangle*, 24.75° N, 121.75° E) in Taiwan

April 15, 2006. The time point of sample collection at the ADS station was at 10:00 in the morning. Water temperature, salinity, and light transmission were measured with a conductivity/temperature/depth recorder (CTD, SBE911 plus, SeaBird). The mixed-layer depth was defined as the water depth within which the density ($\sigma_\theta$) differed from the surface value by <0.1 unit (Gong et al. 1999). Samples from different depths in the water column were collected using 20-L Niskin bottles mounted on the CTD rosette and were further processed for cell enumeration, total RNA extraction, and determinations of chlorophyll *a* and nutrient concentrations as described below.

## Determination of Chlorophyll *a* and Nutrient Concentrations

Seawater sample for chlorophyll *a* analysis was immediately filtered through a 47-mm diameter GF/F filter paper (Whatman), and the filter was frozen in liquid nitrogen until analysis. Chlorophyll *a* retained on the filter was extracted with 90% acetone and was then measured with a fluorometer (Model 10-AU-005, Turner Design). Seawater samples for nutrient analysis were placed in 100-mL polypropylene bottles and immediately frozen in liquid nitrogen. Nitrate concentration was analyzed with a self-designed flow injection analyzer and was reduced to nitrite with a cadmium wire which was activated with a copper sulfate solution. Phosphate concentration was measured by the standard molybdenum blue method. The method employed for chlorophyll *a*, nitrate, and phosphate analyses were described in detail elsewhere (Gong et al. 1996, 2000). Ammonium concentration was determined by the indophenol blue method and further corrected empirically for either pH or salinity (Pai et al. 2001).

## Aerosol Samples and Chemical Analysis of the Dust Composition

A high-volume total suspended particulate aerosol sampler (Tisch Environmental) was set up on the upper foredeck of the ORII. The aerosol particles were continuously filtered onto Whatman-41 cellulose filters (Waterman) for 24 h. Metal ions, including iron and aluminum, in the aerosol particles were analyzed by inductively coupled plasma-mass spectrometry (ICP-MS) (Elan 6100, Perkin Elmer) as described by Hsu et al. (2008, 2010). In addition, hourly averaged dust concentrations (particulate size < 10 μm, $PM_{10}$) at a land-based monitoring station (I-Lan station, 24.75° N, 121.75° E) (Fig. 1) were provided by the Environmental Protection Administration of Taiwan (http://edb.epa.gov.tw/index_air.htm).

## Picophytoplankton Enumeration

Water samples for picophytoplankton enumeration were fixed with paraformaldehyde at a final concentration of 0.2% (*w*/*v*) in the dark for 15 min. These samples were then immediately frozen in liquid nitrogen and kept at −80°C until flow cytometric enumeration (LSR 6, Becton Dickinson). Under excitation at 488 nm, populations of *Synechococcus* and *Prochlorococcus* were distinguished by side scattering and their autofluorescence in the orange (from phycoerythrin, 575 ± 15 nm) and red (from chlorophyll and divinyl chlorophyll, >670 nm) range, respectively (Liu et al. 1995). Furthermore, a known amount of fluorescent beads (TruCOUNT Tubes, Becton Dickinson) was simultaneously counted to calculate the original cell abundance in a sample.

## Total RNA Extraction

Two liters of seawater was prefiltered through 20-μm mesh nylon netting, and cells in the filtrate were then collected on a 47-mm diameter, 0.8-μm pore size polycarbonate membrane (Nucleopore, Whatman) under low pressure (<100 mmHg) within 10 min. Subsequently, a total of six membranes (12-L seawater sample) at a time point were immediately frozen and kept in liquid nitrogen until total RNA extraction. Total RNA was isolated using an RNeasy Plant Mini Kit (Qiagen) according to the manufacturer's instructions. Three membranes (equivalent to a 6-L water sample) were immersed in 1 mL of lysis buffer (RLT buffer, Qiagen) containing 1% β-mercaptoethanol (Merck). Cells were subsequently disrupted by a Mini-Bead Beater (BioSpec) with a proper amount of acid-washed glass

beads (0.1 mm in diameter) (BioSpec). After removing any debris and glass beads by centrifugation, total RNA in the supernatant was isolated using a silica membrane column (Qiagen). Contamination by genomic DNA in the lysate was removed by on-column treatment with RNase-Free DNase I (Qiagen) at room temperature for 30 min. After several washes to remove the DNase and residual salts in the column, total RNA was eluted by an appropriate volume of diethylpyrocarbonate-treated water. The total RNA concentration and purity were determined with a spectrophotometer (ND-1000, NanoDrop Technologies) at wavelengths of 260 and 280 nm.

### Reverse-Transcription Reaction

A suitable amount of DNase I-treated total RNA (100 ng for 16S rRNA cloning and 1 μg for gene expression assays) was reverse-transcribed to first-strand complementary DNA using random hexamers and Improm II reverse transcriptase (Promega). The reaction mixture was incubated at 25°C for 10 min, 48°C for 1 h, and finally at 95°C for 5 min.

### Sequencing and Phylogenetic Analysis of 16S rRNA

To determine the 16S rRNA sequences, 1 μL of complementary DNA (cDNA) was used in a polymerase chain reaction (PCR) with the addition of a high-fidelity DNA polymerase mixture (Advantage II, Clontech). The reaction mixture contained 1× Advantage II buffer, 250 μM dNTP, and 500 nM each of the forward (oxy107F) and reverse primers (oxy1313R) (Table 1) (West et al. 2001). The touch-down PCR conditions were set as follows: 94°C for 2 min for 1 cycle; 94°C for 20 s, 66°C for 20 s, and 68°C for 1.5 min for 5 cycles; 94°C for 20 s, 64°C for 20 s, and 68°C for 1.5 min for 5 cycles; 94°C for 20 s, 62°C for 20 s, and 68°C for 1.5 min for another 25 cycles; and finally at 68°C for 10 min for 1 cycle. The PCR product was further purified with a QIAquick PCR Purification Kit (Qiagen), ligated into the pGEM-T vector (Promega), and transformed into *Escherichia coli* (strain JM109). DNA sequencing of the cloned fragments was performed using an ABI Prism 3730 DNA sequencer (Applied Biosystems). The DNA sequences were further analyzed using Lasergene software (DNASTAR). The BLASTN algorithm from the National Center for Biotechnology Information website (http://www.ncbi.nlm.nih.gov) was also used for sequence annotation. Multiple alignments of 16S rRNA sequences were performed using ClustalW (Chenna et al. 2003), and the phylogenetic tree was constructed by a neighbor-joining analysis with the Jukes–Cantor method (Jukes and Cantor 1969). Programs in the Phylogeny Inference Package (PHYLIP ver. 3.6, distributed by Felsenstein; Department of Genome Sciences, University of Washington, Seattle, USA) were used for the phylogenetic-related analysis and tree construction. All sequences were deposited in the GenBank database with accession numbers FJ903196 to FJ903235 and FJ903236 to FJ903280 for samples collected on March 16 and 18, respectively.

### Determination of the Messenger RNA Levels of Nutrient Deficiency Indicators

A real-time quantitative reverse-transcription polymerase chain reaction (Q-RT-PCR) was conducted to determine the messenger RNA (mRNA) levels of three nutrient deficiency indicator genes, *idiA*, *ntcA*, and *pstS*, in prokaryotic picoplanktonic cells. Q-RT-PCRs were initiated by adding the cDNA fragments to 1× SYBR Green PCR master mix (Applied Biosystems) containing 300 nM each of the forward and reverse primers. Sequences of the primer sets specific to *idiA*, *ntcA*, and *pstS* in the Q-RT-PCR analysis are listed in Table 1 (see next paragraph for verification of the primer specificities). The reactions were then performed on a GeneAmp 7000 sequence detection system (Applied Biosystems). PCR conditions were set to 95°C for 10 min for 1 cycle; and 95°C for 15 s and 60°C for 1 min for 40 cycles. The threshold cycle ($C_T$) at which the fluorescence intensity exceeded a preset threshold was used to calculate the target gene mRNA expression level with a calibration curve constructed by obtaining $C_T$ values from a series of standards containing known amounts of the target gene DNA fragments. The standards were obtained by PCR

**Table 1** The primer sets used in the phylogenetic analysis of 16S rRNA and the quantification of mRNA levels of the nutrient starvation-related genes

| Target gene | Primer name | Sequence (5′→3′) | Amplicon (bp) |
|---|---|---|---|
| 16S rRNA (West et al. 2001) | oxy-107F<br>oxy-1313R | ggacg ggtga gtaac gcgtr a<br>cttca cgtag gcgag ttgca gc | 1,147 |
| *idiA* | idiA-SG-F<br>idiA-SG-R | gatgc tgaat ccaga caagg ttc<br>gactg gttgt aaacg ctttt gcg | 117 |
| *ntcA* | ntcA-SG-F<br>ntcA-SG-R | carac sgara csatg atyga gac<br>gkgtg gancc ratgg cytcg gc | 165 |
| *pstS* | pstS-SG-F<br>pstS-SG-R | tccca gccaa gatct accag c<br>ctggt cgatg aaagc cttac g | 113 |

r = a or g; k = g or t; s = g or c; y = c or t; n = a or g or t or c

reactions, using the plasmids containing *idiA*, *ntcA*, and *pstS* gene fragments of *Synechococcus* WH7803 as templates. Subsequently, the target gene mRNA expression levels were normalized to the estimated cell number in the sample for total RNA extraction and the amount of total RNA in RT reaction given above.

### Specificities of the Primer Pairs of Nutrient Deficiency Indicators

The *idiA*, *ntcA*, and *pstS* primer pairs for *Synechococcus* were designed based on the alignment results of the full-length nucleotide sequences. These sequences were obtained from the samples collected at the ADS station and from the GenBank database. The specificities of *idiA*, *ntcA*, and *pstS* primer pairs applied in the Q-RT-PCR assays were examined by three independent procedures (Fan 2006; Hung 2009). (1) Using the total RNA extracted from unialgal cultures, these primer pairs were able to specifically amplify each target cDNA in the *Synechococcus* strains, WH6501 (clade II) and WH7803 (clade V), but failed in the *Prochlorococcus* strains, MIT9301 (high-light clade), MED4 (high-light clade), and NATL1A (low-light clade). (2) Homogeneity in amplicon size composition was confirmed by both melting temperature analysis and electrophoresis on 3% agarose gels. The melting temperature analysis was performed on a GeneAmp 7000 sequence detection system (Applied Biosystems) with the temperature increasing from 65°C to 95°C over 20 min at the completion of the Q-RT-PCR. (3) The correctness of the mRNA of these three genes detected in field samples was further confirmed by the nucleotide sequencing of the amplicons. Results from these procedures indicated that the primers listed in Table 1 can reliably determine the mRNA levels of *idiA*, *ntcA*, and *pstS* in *Synechococcus* cells at our study site.

## Results

### Cell Abundances of Picophytoplankton

From March 15 to April 15, 2006, five cruises were conducted to investigate the effects of ADSs on the ecosystem in a subtropical segment of the Kuroshio Current (Fig. 1). In this study, a total aerosol aluminum (Al) concentration of 1,500 ng $m^{-3}$ was adopted as a criterion for identifying the occurrence of a significant ADS event (Hsu et al. 2008). Accordingly, three significant ADS events were identified on March 18 (cruise 1), March 29 to 30 (cruise 3), and April 9 (cruise 4) (Fig. 2a). In addition, another likely significant ADS event ($PM_{10}$ > 100 μg $m^{-3}$) (Liu et al. 2006) occurred on April 3, which was recorded at the I-Lan station of Taiwan's EPA, but no cruise was conducted and the aerosol Al was not measured (Fig. 2a). During the period of cruise 1, the total Al concentration reached a high level of 5,891 ng $m^{-3}$ on March 18, and a heavy dust load was also observed at the I-Lan station the following day. However, the mixed-layer depths remained at 24 to 49 m, indicating that the turbulence was not especially strong (Fig. 2b). Cell numbers of *Synechococcus* showed a significant increase of nearly 10-fold from 1.4 × $10^4$ to 1.0 × $10^5$ cells $mL^{-1}$ during the period from March 16 to 18, and then declined to 4.1 × $10^4$ cells $mL^{-1}$ on March 19 (Fig. 2c). Meanwhile, the chlorophyll *a* concentrations also increased in a similar pattern (Fig. 2d). Accompanying the peak of Al loading, the amount of soluble Fe in the dust reached the highest level of 54.8 ng $m^{-3}$ on March 18 (Fig. 2e). The total nitrogen ($NH_4$ + $NO_3$) and inorganic phosphate concentrations in surface water remained low on March 18, but had increased to high values of 870 and 210 nM, respectively, on March 19 (Fig. 2f, g).

According to the Al and $PM_{10}$ concentrations monitored at the I-Lan station, two consecutive ADS events occurred between March 27 and April 6. Because weather conditions were unfavorable during cruise 3, onboard observations lasted for only 2 days during the period. On March 29, the highest Al concentration in the dust exceeded 7,000 ng $m^{-3}$, and the mixed layer at the ADS station also deepened to 127 m in depth (Fig. 2a, b). The abundance of *Synechococcus* doubled from 2.1 × $10^4$ to 4.1 × $10^4$ cells $mL^{-1}$ in a period of 24 h (Fig. 2c).

During cruises 4 and 5, a weak ADS event (based on the Al concentration) occurred on April 9, but no intensified water mixing was observed at the ADS station (Fig. 2a, b). The amount of soluble Fe in the dust was around 20 ng $m^{-3}$ (Fig. 2e). In surface water, a high value of the $NH_4$ concentration of 670 nM was observed on April 11 (Fig. 2f). Cell numbers of *Synechococcus* increased from 2.8 × $10^4$ (April 7) to 8.3 × $10^4$ cells $mL^{-1}$ (April 11), representing an increase of about 3-fold (Fig. 2c). The chlorophyll *a* concentration also reached a high value of 0.69 mg $m^{-3}$ (Fig. 2d). Furthermore, the abundance of the *Prochlorococcus* showed a significant decline from 2.8 × $10^5$ to 1.1 × $10^5$ cells $mL^{-1}$, in contrast to the enhancement of *Synechococcus* cell numbers (Fig. 2c).

### Genetic Diversity of *Synechococcus* and *Prochlorococcus*

During cruise 1, *Synechococccus* cell numbers dramatically increased with the developing ADS event, and a phylogenetic analysis of 16S rRNA sequences revealed a shift in the community structure of picophytoplankton. In the sample collected on March 16, 43 sequences were obtained with 3 sequences apparently belonging to heterotrophic

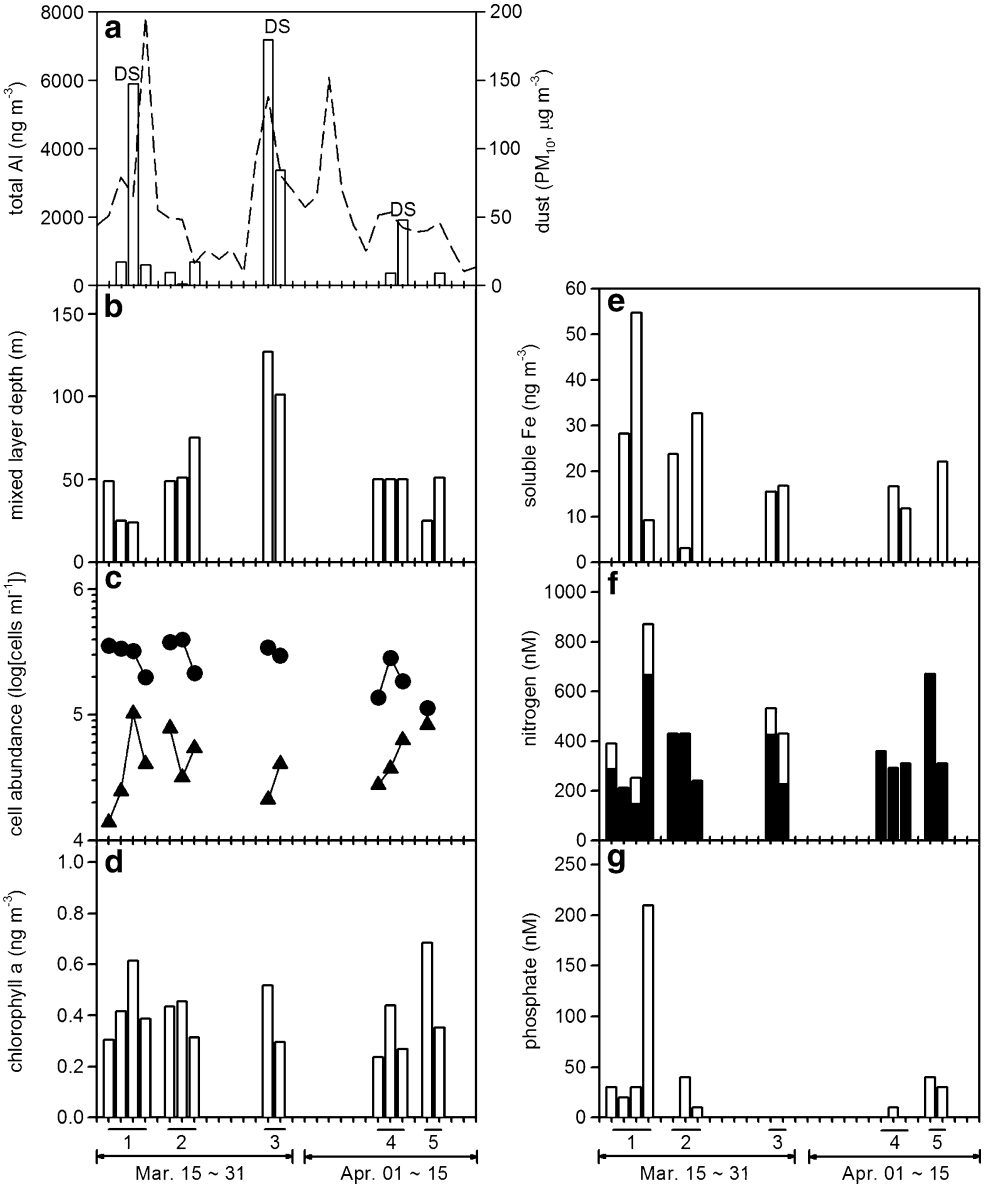


**Fig. 2** Time courses of various environmental and biological parameters at the Asian Dust Storm (ADS) station. **a** Total aerosol Al concentration (*open bars*) measured onboard (Hsu et al. 2010) and the $PM_{10}$ concentration (*dashed line*) monitored at the I-Lan land-based station of Taiwan's EPA. The identification of a dust storm (DS) event was based on a total Al concentration of >1,500 ng $m^{-3}$ (Hsu et al. 2008). **b** Mixed-layer depths at the ADS station. **c** Abundances of *Prochlorococcus* (*circles*) and *Synechococcus* (*triangles*). **d** Concentration of chlorophyll *a* in surface water. **e** Concentration of soluble Fe associated with dust particles (Hsu et al. 2010). **f** Nutrient concentrations of $NH_4$ (*filled bars*) and $NO_3$ (*open bars*) in the 3-m deep surface waters. **g** Concentration of inorganic phosphate in surface waters. The durations of five cruises are marked below panels **d** and **g**. Cruise 1: March 16–19; cruise 2: March 21–23; cruise 3: March 29–30; cruise 4: April 7–9; cruise 5: April 11–12

bacteria. The rest of them were cyanobacterial picoplankton sequences. A majority of this group were categorized as *Prochlorococcus* sequences, including 22 sequences belonging to high-light I and II (HL I and HL II) ecotypes, 1 sequence belonging to the low-light (LL) ecotype, and the other 3 sequences (031606#14, #30, and #36) that did not group with any of the known ecotypes. Moreover, the other 14 sequences were categorized as *Synechococcus*. Within this group, eight sequences were distributed more or less evenly among clades II, III, VII, and X. However, six *Synechococcus* sequences (031606#1, #16, #28, #32, #35, and #39) were not associated with any of the known clades. In summary, *Prochlorococcus* was the more abundant group among the picophytoplankton, and no dominant clade of *Synechococcus* was observed on March 16 (Fig. 3, Table 2). This pattern, however, dramatically changed on March 18. Of the 46 sequences obtained, most showed high identities to 16S rRNA sequences of *Synechococcus*, including 21 sequences belonging to *Synechococcus* clade II, and 7 sequences belonging to clade III. In contrast, only 11 sequences belonged to *Prochlorococcus*, including 7 sequences of HL I and HL II, and the other 4 sequences (031806#8, #17, #21, #35) failed to associate with any known ecotypes (Fig. 4, Table 2). Consequently, the clade II genotype became the dominant lineage in the newly emerged *Synechococcus* community (Table 2).

## Expressions of Nutrient Deficiency Indicators

During cruise 1 (March 16 to 19), the mRNA levels of three nutrient starvation-related genes, *idiA*, *ntcA*, and *pstS*, were used to evaluate the status of nutrient sufficiency in

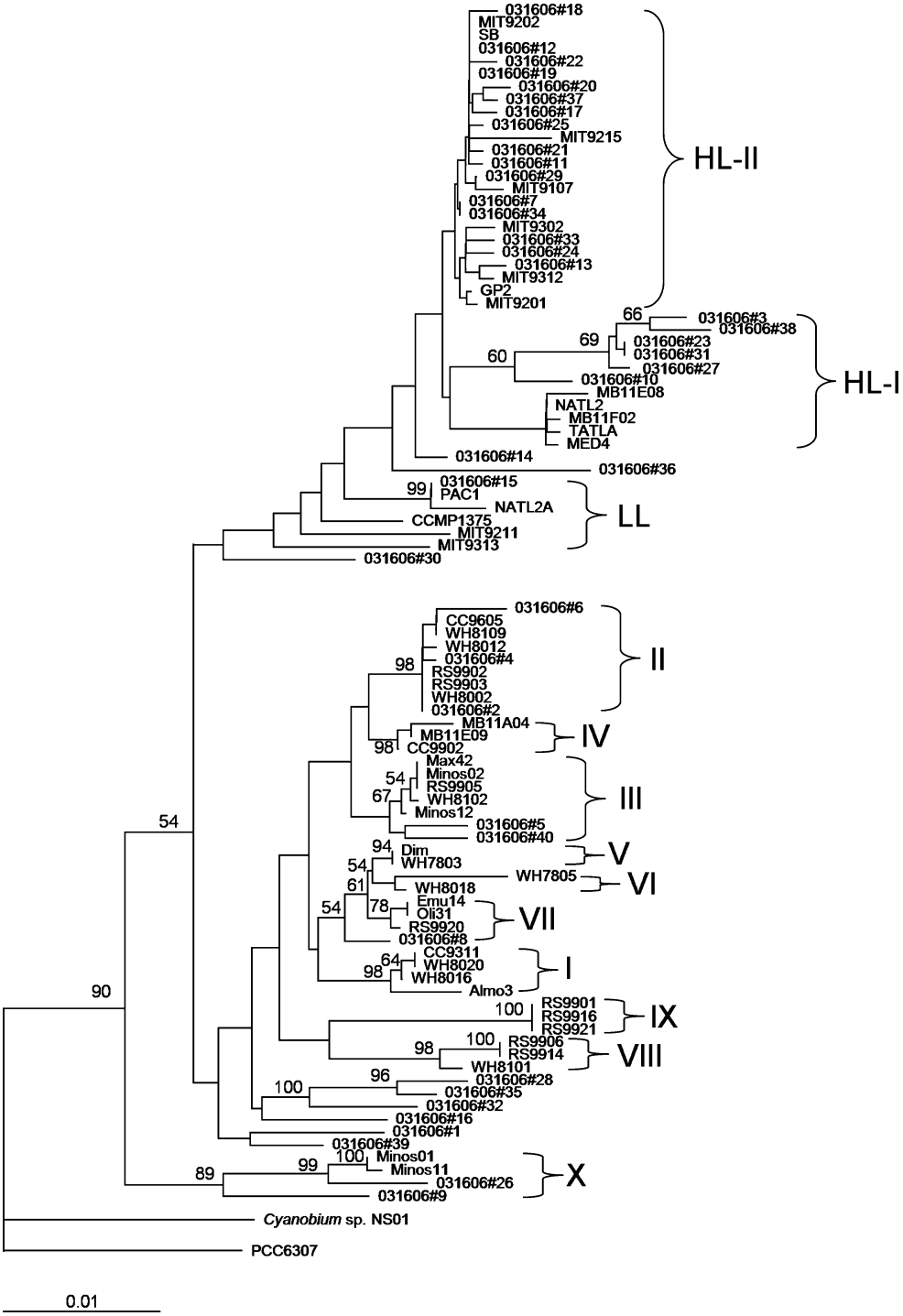


**Fig. 3** Neighbor-joining phylogenetic tree inferred from 16S rRNA sequences of *Prochlorococcus* and *Synechococcus* at the ADS station on March 16, 2006. The ecotypes of *Prochlorococcus* and the 10 clade lineages of *Synechococcus* are denoted on the *right* (Fuller et al. 2003; Rocap et al. 2003). The effects of sampling error on the tree inference and the stability of branch nodes were tested by a bootstrap analysis with 1,000 repetitions. Bootstrap values of >50% are presented on the branches. The freshwater strain of *Synechococcus* PCC6307 served as the root. The length of the scale bar on the *lower left* indicates 0.01 nucleotide substitution units. The sequence obtained from surface water at the ADS station was denoted by the sample date and clone number. All sequences were deposited in the GenBank database with accession numbers FJ903196 to 235. All sequences of identified strains were obtained from the GenBank database

*Synechococcus*. In surface waters (3 m in depth) at the ADS station, the mRNA levels of *ntcA* increased from 4.9 to 133.7 copies cell$^{-1}$ between March 16 and 18 and had decreased to 2.4 copies cell$^{-1}$ by March 19. A similar trend was observed for cell numbers of *Synechococcus* (Fig. 5a, b). On the other hand, the mRNA abundance of *idiA* was at a relatively high value of 5.3 copies cell$^{-1}$ on March 17, which had decreased to 1.8 copies cell$^{-1}$ on March 18, and finally declined to a non-detectable level on March 19 (Fig. 5c). Similarly, the mRNA abundance of *pstS* also showed a decreasing trend from 19.1 copies cell$^{-1}$ on March 17 to a non-detectable level on March 19 (Fig. 5d). At 50 m in depth, cell numbers of *Synechococcus* steadily increased from 1.2 × $10^4$ to 4.4 × $10^4$ cells mL$^{-1}$, representing a 4-fold increase within 48 h (Fig. 5a). Meanwhile, all three nutrient deficiency indicators showed

**Table 2** The succession of dominant prokaryotic picoplankton as analyzed by the phylogenesis of 16S rRNA sequences at the ADS station during Cruise 1 (March 16 to 18, 2006)

| Date | *Synechococcus* | | *Prochlorococcus* | | Heterotrophic bacteria | Clone number |
|---|---|---|---|---|---|---|
| | Clade II | Other clades | HL I & II | Other ecotypes | | |
| March 16 | 3 (7.0%) | 11 (25.6%) | 24 (55.8%) | 2 (4.6%) | 3 (7.0%) | 43 (100%) |
| March 18 | 21 (45.7%) | 12 (26.1%) | 7 (15.2%) | 4 (8.7%) | 2 (4.3%) | 46 (100%) |

The percentage of 16S rRNA sequence belonging to a specific clade is included in parenthesis

increased expressions (Fig. 5b–d). The mRNA abundances of *ntcA* increased from 0.2 to 26.6 copies cell$^{-1}$, representing an increase of about 100-fold within 24 h (Fig. 5b). In addition, the mRNA levels of *idiA* and *pstS* increased from 1.5 to 34.9 copies cell$^{-1}$ and from 4.1 to 16.4 copies cell$^{-1}$, respectively (Fig. 5c, d). The mRNA levels of *idiA*, *ntcA*, and *pstS* were undetectable in the samples collected from the other four cruises.

## Discussion

Vigorous growth of *Synechococcus* was observed in surface waters at our study site accompanying the occurrences of ADS events. This observation indicated that ADS caused a similar response in the subtropical Kuroshio Current as those reported for dust storms in other marine ecosystems. For example, dust deposition from the Sahara Desert stimulated short-term growth of *Synechococcus* in oligotrophic waters of the tropical North Atlantic and Mediterranean Sea (Davey et al. 2008; Herut et al. 2005; Zohary et al. 2005). In cruise 1, the heavy load of dust particles was probably the main factor resulting in the transient *Synechococcus* bloom because no obvious mixing occurred (Fig. 2a–c). Additionally, the expression profiles of nutrient starvation-related genes supported this speculation (Fig. 5). Apparent declines in *ntcA* and *pstS* expressions and low *idiA* mRNA levels indicated that nutrients from atmospheric deposition were sufficient to trigger vigorous growth of *Synechococcus* in surface waters. At a greater depth (50 m), although the abundance of *Synechococcus* still increased with time, the high mRNA levels of *idiA* and *pstS* implied that *Synechococcus* cells were experiencing iron and phosphorus starvation.

The elevated mRNA level of *ntcA* on March 18 was not necessarily in conflict with the conclusion that nutrients were sufficient and *Synechococcus* grew actively during this ADS event (Fig. 5a, b). In the absence of $NH_4$, *ntcA* expression is enhanced to upregulate other genes that are subsequently required to utilize other forms of nitrogenous compounds (Luque et al. 1994; Lindell and Post 2001). Consequently, the dramatic increase in *ntcA* mRNA levels on March 18 implied that ambient $NH_4$ was exhausted, and the growth of *Synechococccus* was probably maintained by an alternative form of nitrogen. Subsequently on March 19, the decline in *Synechococcus* abundance and the appearance of high $NH_4$ concentrations in surface waters led to the decrease in *ntcA* mRNA to an undetectable level (Figs. 2f and 5b).

In addition to the dust load, nutrients supplied by deep-water mixing was another factor that might induce the growth of *Synechococcus* in surface waters (Lindell and Post 1995; DuRand et al. 2001; Herut et al. 2005; Yuan and Zhang 2006). A series of ADS events was observed at the I-Lan station from March 27 to April 6. Strong turbulence was also observed from March 29 to 30. It is likely that the heavy dust load and the strong vertical mixing jointly injected large amounts of nutrients into surface waters and led to the formation of the *Synechococcus* bloom during the period from March 29 to 30. A similar bloom may have occurred on April 2 to 5, but this phenomenon could not be studied onboard because of the rough sea state. In addition, residual nutrients in surface waters provided by these two ADS events probably stimulated the rapid growth of *Synechococcus* between April 7 and 11.

When an ADS stimulated *Synechococcus* to bloom, the cell abundance of *Prochlorococcus* showed little variation, and a weak decline usually followed the plateau phase (Fig. 2c). Differences between temporal patterns of *Synechococcus* and *Prochlorococcus* were also observed in the East Mediterranean (Herut et al. 2005). Although the small cell size of *Prochlorococcus* is advantageous in competing for nutrients in an extremely oligotrophic ocean, *Synechococcus* is more versatile in utilizing diverse nitrogenous compounds (Glover et al. 1988; Moore et al. 2002; Rocap et al. 2003). Furthermore, *Synechococcus* has higher maximum uptake rates and affinities for orthophosphate than do other phytoplankton (Moutin et al. 2002). As a result, the abrupt input of external nutrients would preferentially cause *Synechococcus* to grow (Herut et al. 2005; Post 2005). Additionally, *Prochlorococcus* seems more sensitive to toxic compounds released from atmospheric deposition, which gives *Synechococcus* a better chance to bloom (Mann et al. 2002). However, Paytan et al.

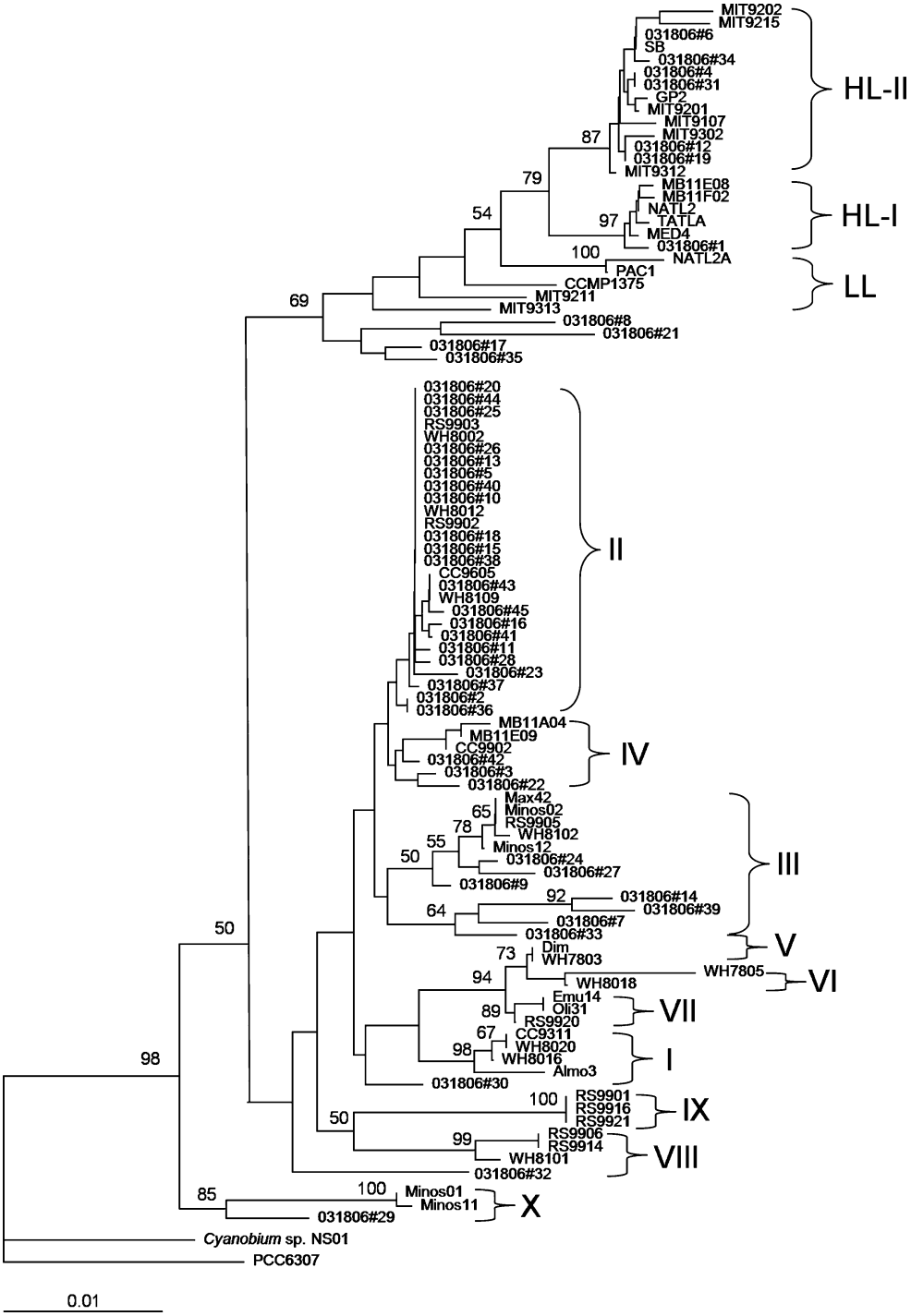


**Fig. 4** Neighbor-joining phylogenetic tree inferred from 16S rRNA sequences of *Prochlorococcus* and *Synechococcus* at the ADS station on March 18, 2006. All sequences were deposited in the GenBank database with accession numbers FJ9032 to 80. Other descriptions are the same as in the legend of Fig. 3

(2009) have opposite views on that *Prochlorococcus* showed higher tolerance on the toxicity of copper from the aerosol.

Diatoms are the larger phytoplankton species that show early responses to the loadings of new nutrients (Goldman 1993). This response has been well documented in iron fertilization experiments conducted in the high-nitrate low-chlorophyll oceans (Coale et al. 1996; Boyd et al. 2000, 2005). After the ADS event occurred in cruise 1, we found that diatoms thrived from 0.4 to 3.0 × $10^4$ cells $L^{-1}$. DiTullio and Laws (1991) also reported the concentration of fucoxanthin, the characteristic pigment of diatoms, in North Pacific Central Gyre increased as a result of the ADS disturbances. Moreover, the rise of zooplankton biomass, accompanied with energetic grazing and metabolism, was observed immediately after a Sahara dust-induced bloom (Hernández-León et al. 2004). Intensive grazing will transform considerable POC inventory into POC export

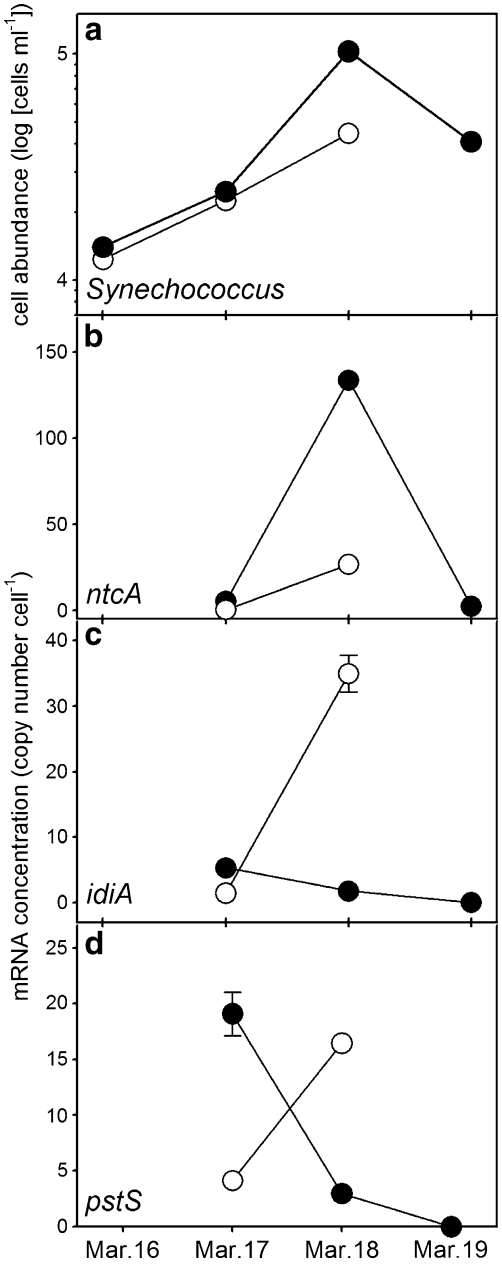


**Fig. 5** Time courses of **a** *Synechococcus* abundances, and **b** *ntcA*, **c** *idiA*, and **d** *pstS* mRNA levels in surface and deep waters at the Asian dust storm (ADS) station during cruise 1 (March 16–19, 2006). The data points obtained from depths of 3 and 50 m are denoted by *solid* and *open circles*, respectively. *Error bars* in panels **b**, **c**, and **d** indicate standard errors ($n$ = 3). For data points without an error bar, the error bar was smaller than the symbol

flux, which provides a good explanation for the close connection between POC export flux and dust deposition (Neuer et al. 2004; Hung et al. 2009).

Within *Synechococcus*, not all lineages respond equally to dust storms. Based on 16S rRNA gene sequences, all 10 clades belonging to the marine *Synechococcus* subcluster 5.1 (Fuller et al. 2003; Scanlan et al. 2009) were observed with no dominant clade at our study site prior to the arrival of an ADS event on March 18, 2006. At the peak of the ADS event, however, clade II sequences had increased and contributed more than 45% to the *Synechococcus* community (Table 2). According to the global distribution pattern of *Synechococcus*, clade II was suggested to be a dominant lineage in upwelling, coastal, and continental shelf zones between the latitudes of 30° S and 30° N (Zwirglmaier et al. 2007, 2008). Our results suggested that a temporary nutrient enrichment in an oligotrophic ocean resulted in the rapid growth of *Synechococcus* clade II and changed the genetic composition of the cyanobacterial picophytoplankton (Figs. 4 and 5). Although nutrient requirements among the different clade lineages of *Synechococcus* still need to be clarified, clade II seems to be a good indicator of nutrient-related environmental changes in oligotrophic regions.

In the phylogenetic analysis, several 16S rRNA sequences failed to associate with known groups of cyanobacterial picoplankton in spite of the fact that they showed high identity scores with some uncultured picoplankton from equatorial Atlantic Ocean and the South China Sea. This result implied that the present classification system of cyanobacterial picoplankton based on the 16S rRNA sequences is still incomplete. A possible cause might be that the majority of sequences used to construct the current view of 16S rRNA gene diversity came from several oceanic provinces, such as the Red Sea, Atlantic Ocean, and Southeast Pacific Ocean, for decades (Fuller et al. 2003; Zwirglmaier et al. 2007, 2008), but relatively few sequences were from the Northwest Pacific Ocean. The determination of the phylogenetic associations for these unclassified sequences in the subtropical Kuroshio Current will rely on some newly developed high-throughput sequencing techniques such as the one described in Delong (2009).

Although *idiA*, *ntcA*, and *pstS* have been successfully employed to clarify nutrient assimilation status of *Synechococcus* in several oceanic provinces, comparisons of transcript abundances between various isolated strains and between cultured and natural populations are seldom discussed. By the use of *Synchococcus* WH7803 (clade V) as a model organism, we evaluated the mRNA expression level of *pstS* was 25 copies cell$^{-1}$ under phosphate limitation. This result coincided with the estimation in the ADS event (Fig. 5d). Nevertheless, in contrast to *pstS*, the mRNA abundances of *idiA* and *ntcA* in iron- and nitrogen-depleted cultures were 0.5 and 37 copies cell$^{-1}$, respectively, which were significantly less than the high values observed in the field (Fig. 5b, c). It is probably due to the different primer affinities for individual *Synechococcus* lineages. This kind of variation has been reported in the absolute quantification protocol of real-time Q-RT-PCR (Smith and Osborn 2009). Under this

circumstance, we are confident that the trends of variations in mRNA abundances are reliable. However, the accuracy of the absolute copy numbers per cell needs to be confirmed by testing additional *Synechococcus* isolates, as well as a larger group of nutrient deficiency indicator sequences collected from the Kuroshio Current.

In summary, our results elucidated that the clade II lineage of *Synechococcus* thrived in the oligotrophic Kuroshio under the influences of ADS events. As a result, this group of organisms became the most abundant picophytoplankton in a habitat typically dominated by *Prochlorococcus*. Such a change was jointly stimulated by large amounts of nutrients, including nitrogen, phosphorus, and iron, provided by aeolian deposition and strong mixing which accompanies ADS events. The fate of such increased picophytoplankton biomass and related issues in population dynamics deserve further research.

**Acknowledgments** We are grateful to the Core Facility of the Institute of Cellular and Organismic Biology, Academia Sinica, for assistance with DNA sequencing. This study was supported by grants (NSC95-2611-M-019-018-MY3, NSC96-2811-M-019-001, NSC98-2611-M-019-007-MY3, NSC 98-2611-M-019-014-MY3, and NSC98-2611-M-019-006) from the National Science Council (Taiwan) and a grant from the Center for Marine Bioenvironment and Biotechnology, National Taiwan Ocean University.

## References

Bishop JKB, Davis RE, Sherman JT (2002) Robotic observations of dust storm enhancement of carbon biomass in the North Pacific. Science 298:817–821

Blanchot J, Rodier M (1996) Picophytoplankton abundance and biomass in the western tropical Pacific Ocean during the 1992 El Nino year: results from flow cytometry. Deep Sea Res I 43:877–895

Boyd PW, Watson AJ, Law CS, Abraham ER, Trull T, Murdoch R, Bakker DCE, Bowie AR, Buesseler KO, Chang H, Charette M, Croot P, Downing K, Frew R, Gall M, Hadfield M, Hall J, Harvey M, Jameson G, LaRoche J, Liddicoat M, Ling R, Maldonado MT, McKay RM, Nodder S, Pickmere S, Pridmore R, Rintoul S, Safi K, Sutton P, Strzepek R, Tanneberger K, Turner S, Waite A, Zeldis J (2000) A mesoscale phytoplankton bloom in the polar Southern Ocean stimulated by iron fertilization. Nature 407:695–702

Boyd PW, Strzepek R, Takeda S, Jackson G, Wong CS, McKay RM, Law C, Kiyosawa H, Saito H, Sherry N, Johnson K, Gower J, Ramaiah N (2005) The evolution and termination of an iron-induced mesoscale bloom in the northeast subarctic. Pac Limnol Oceanogr 50:1872–1886

Boyd PW, Jickells T, Law CS, Blain S, Boyle EA, Buesseler KO, Coale KH, Cullen JJ, de Baar HJW, Follows M, Harvey M, Lancelot C, Levasseur M, Owens NPJ, Pollard R, Rivkin RB, Sarmiento J, Schoemann V, Smetacek V, Takeda S, Tsuda A, Turner S, Watson AJ (2007) Mesoscale iron enrichment experiments 1993–2005: synthesis and future directions. Science 315:612–617

Campbell L, Vaulot D (1993) Photosynthetic picoplankton community structure in the subtropical North Pacific Ocean near Hawaii (station ALOHA). Deep Sea Res 40:2043–2060

Chenna R, Sugawara H, Koike T, Lopez R, Gibson TJ, Higgins DG, Thompson JD (2003) Multiple sequence alignment with the Clustal series of programs. Nucleic Acids Res 31:3497–3500

Chiang K-P, Kuo M-C, Chang J, Wang R-H, Gong G-C (2002) Spatial and temporal variation of the *Synechococcus* population in the East China Sea and its contribution to phytoplankton biomass. Cont Shelf Res 22:3–13

Chisholm SW, Olson RJ, Zettler ER, Goericke R, Waterbury JB, Welschmeyer NA (1988) A novel free-living prochlorophyte abundant in the oceanic euphotic zone. Nature 334:340–343

Coale KH, Johnson KS, Fitzwater SE, Gordon RM, Tanner S, Chavez FP, Ferioli L, Sakamoto C, Rogers P, Millero F, Steinberg P, Nightingale P, Cooper D, Cochlan WP, Landry MR, Constantinou J, Rollwagen G, Trasvina A, Kudela R (1996) A massive phytoplankton bloom induced by an ecosystem-scale iron fertilization experiment in the equatorial Pacific Ocean. Nature 383:495–501

Davey M, Tarran GA, Mills MM, Ridame C, Geider RJ, La Roche J (2008) Nutrient limitation of picophytoplankton photosynthesis and growth in the tropical North Atlantic. Limnol Oceanogr 53:1722–1733

DeLong EF (2009) The microbial ocean from genomes to biomes. Nature 459:200–206

DiTullio GR, Laws EA (1991) Impact of an atmospheric–oceanic disturbance on phytoplankton community dynamics in the North Pacific Central Gyre. Deep Sea Res 38:1305–1329

DuRand MD, Olson RJ, Chisholm SW (2001) Phytoplankton population dynamics at the Bermuda Atlantic time-series station in the Sargasso Sea. Deep Sea Res II 48:1983–2003

Falkowski P, Scholes RJ, Boyle E, Canadell J, Canfield D, Elser J, Gruber N, Hibbard K, Hogberg P, Linder S, Mackenzie FT, Moore B III, Pedersen T, Rosenthal Y, Seitzinger S, Smetacek V, Steffen W (2000) The global carbon cycle: a test of our knowledge of earth as a system. Science 290:291–296

Fan TP (2006) The diversity of iron deficiency induced protein A gene (*idiA*) and nitrogen control gene A (*ntcA*) in the East China Sea and its application to the design of specific primers. MS dissertation. Institute of Marine Biology. Keelung: National Taiwan Ocean University

Fuller N, Marie D, Partensky F, Vaulot D, Post A, Scanlan D (2003) Clade-specific 16S ribosomal DNA oligonucleotides reveal the predominance of a single marine *Synechococcus* clade throughout a stratified water column in the Red Sea. Appl Environ Microbiol 69:2430–2443

Fuller NJ, West NJ, Marie D, Yallop M, Rivlin T, Post AF, Scanlan DJ (2005) Dynamics of community structure and phosphate status of picocyanobacterial populations in the Gulf of Aqaba, Red Sea. Limnol Oceanogr 50:363–375

Glover HE, Prezelin BB, Campbell L, Campbell M, Garside C (1988) A nitrate-dependent *Synechococcus* bloom in surface Sargasso Sea water. Nature 331:161–163

Goericke R, Welschmeyer NA (1993) The marine prochlorophyte *Prochlorococcus* contributes significantly to phytoplankton biomass and primary production in the Sargasso Sea. Deep Sea Res I 40:2283–2294

Goldman JC (1993) Potential role of large oceanic diatoms in new primary production. Deep Sea Res I 40:159–168

Gong G-C, Chen Y-L, Liu K-K (1996) Summertime hydrography and chlorophyll *a* distribution in the East China Sea in summer: implications of nutrient dynamics. Cont Shelf Res 16:1561–1590

Gong G-C, Shiah F-K, Liu K-K, Chuang W-S, Chang J (1997) Effect of the Kuroshio intrusion on the chlorophyll distribution in the southern East China Sea during spring 1993. Cont Shelf Res 17:79–94

Gong G-C, Chang J, Wen Y-H (1999) Estimation of annual primary production in the Kuroshio waters northeast of Taiwan using a photosynthesis-irradiance model. Deep Sea Res I 46:93–108

Gong G-C, Shiah F-K, Liu K-K, Wen Y-H, Liang M-H (2000) Spatial and temporal variation of chlorophyll *a*, primary productivity and chemical hydrography in the southern East China Sea. Cont Shelf Res 20:411–436

Goudie AS, Middleton NJ (2001) Saharan dust storms: nature and consequences. Earth Sci Rev 56:179–204

Hernández-León S, Almeida C, Bécognée P, Yebra L, Arístegui J (2004) Zooplankton biomass and indices of grazing and metabolism during a late winter bloom in subtropical waters. Mar Biol 145:1191–1200

Herut B, Zohary T, Krom MD, Mantoura RFC, Pitta P, Psarra S, Rassoulzadegan F, Tanaka T, Thingstad TF (2005) Response of East Mediterranean surface water to Saharan dust: on-board microcosm experiment and field observations. Deep Sea Res II 52:3024–3040

Hsu S-C, Liu SC, Huang Y-T, Lung S-CC, Tsai F, Tu J-Y, Kao S-J (2008) A criterion for identifying Asian dust events based on Al concentration data collected from northern Taiwan between 2002 and early 2007. J Geophys Res 113:D18306

Hsu S-C, Liu SC, Arimoto R, Liu T-H, Huang Y-T, Tsai F, Lin F-J, Kao S-J (2009) Dust deposition to the East China Sea and its biogeochemical implications. J Geophys Res 114:D15304

Hsu S-C, Wong GTF, Gong G-C, Shiah F-K, Huang Y-T, Kao S-J, Tsai F, Candice Lung S-C, Lin F-J, Lin II, Hung C-C, Tseng C-M (2010) Sources, solubility, and dry deposition of aerosol trace elements over the East China Sea. Mar Chem 120:116–127

Hung C-C, Gong G-C, Chung W-C, Kuo W-T, Lin F-C (2009) Enhancement of particulate organic carbon export flux induced by atmospheric forcing in the subtropical oligotrophic northwest Pacific Ocean. Mar Chem 113:19–24

Hung S-H (2009) The expression of *pstS* in the East China Sea picoplankton community: primer design and field tests. MS dissertation. Institute of Marine Environmental Chemistry and Ecology. Keelung: National Taiwan Ocean University

Jiao N, Yang Y, Koshikawa H, Watanabe M (2002) Influence of hydrographic conditions on picoplankton distribution in the East China Sea. Aquat Microb Ecol 30:37–48

Jickells TD (1995) Atmospheric inputs of metals and nutrients to the oceans: their magnitude and effects. Mar Chem 48:199–214

Jickells TD, An ZS, Andersen KK, Baker AR, Bergametti G, Brooks N, Cao JJ, Boyd PW, Duce RA, Hunter KA, Kawahata H, Kubilay N, laRoche J, Liss PS, Mahowald N, Prospero JM, Ridgwell AJ, Tegen I, Torres R (2005) Global iron connections between desert dust, ocean biogeochemistry, and climate. Science 308:67–71

Jukes TH, Cantor CR (1969) Evolution of protein molecules. In: Munro HN (ed) Mammalian protein metabolism. Academic, New York, pp 21–132

Katano T, Kaneda A, Kanzaki N, Obayashi Y, Morimoto A, Onitsuka G, Yasuda H, Mizutani S, Kon Y, Hata K, Takeoka H, Nakano S-I (2007) Distribution of prokaryotic picophytoplankton from Seto Inland Sea to the Kuroshio region, with special reference to 'Kyucho' events. Aquat Microb Ecol 46:191–201

Kellogg CA, Griffin DW (2006) Aerobiology and the global transport of desert dust. Trends Ecol Evol 21:638–644

Lindell D, Post AF (1995) Ultraphytoplankton succession is triggered by deep winter mixing in the Gulf of Aqaba (Eilat), Red Sea. Limnol Oceanogr 40:1130–1141

Lindell D, Post AF (2001) Ecological aspects of *ntcA* gene expression and its use as an indicator of the nitrogen status of marine *Synechococcus* spp. Appl Environ Microbiol 67:3340–3349

Lindell D, Penno S, Al-Qutob M, David E, Rivlin T, Lazar B, Post AF (2005) Expression of the nitrogen stress response gene *ntcA* reveals nitrogen-sufficient *Synechococcus* populations in the oligotrophic northern Red Sea. Limnol Oceanogr 50:1932–1944

Liu CM, Young CY, Lee YC (2006) Influence of Asian dust storms on air quality in Taiwan. Sci Total Environ 368:884–897

Liu H, Campbell L, Landry MR (1995) Growth and mortality rates of *Prochlorococcus* and *Synechococcus* measured with a selective inhibitor technique. Mar Ecol Prog Ser 116:277–287

Liu H, Nolla HA, Campbell L (1997) *Prochlorococcus* growth rate and contribution to primary production in the equatorial and subtropical North Pacific Ocean. Aquat Microb Ecol 12:9–47

Luque I, Flores E, Herrero A (1994) Molecular mechanism for the operation of nitrogen control in cyanobacteria. EMBO J 13:2862–2869

Mann EL, Ahlgren N, Moffett JW, Chisholm SW (2002) Copper toxicity and cyanobacteria ecology in the Sargasso Sea. Limnol Oceanogr 47:976–988

Mills MM, Ridame C, Davey M, La Roche J, Geider RJ (2004) Iron and phosphorus co-limit nitrogen fixation in the eastern tropical North Atlantic. Nature 429:292–294

Moore LR, Post AF, Rocap G, Chisholm SW (2002) Utilization of different nitrogen sources by the marine cyanobacteria *Prochlorococcus* and *Synechococcus*. Limnol Oceanogr 47:989–996

Moutin T, Thingstad TF, van Wambeke F, Marie D, Slawyk G, Raimbault P, Claustre H (2002) Does competition for nanomolar phosphate supply explain the predominance of the cyanobacterium *Synechococcus*? Limnol Oceanogr 47:1562–1567

Neuer S, Torres-Padrón M, Gelado-Caballero M, Rueda M, Hernández-Brito J, Davenport R, Wefer G (2004) Dust deposition pulses to the eastern subtropical North Atlantic gyre: does ocean's biogeochemistry respond? Glob Biogeochem Cycles 18:GB4020

Nitani H (1972) Beginning of the Kuroshio. In: Stommel H, Yoshida K (eds) Kuroshio. University of Washington Press, Seattle, pp 129–163

Pai S-C, Tsau Y-J, Yang T-I (2001) pH and buffering capacity problems involved in the determination of ammonia in saline water using the indophenol blue spectrophotometric method. Anal Chim Acta 434:209–216

Partensky F, Blanchot J, Vaulot D (1999a) Differential distribution and ecology of *Prochlorococcus* and *Synechococcus* in oceanic waters: a review. Bull Inst Océanogr Monaco 19:457–475

Partensky F, Hess WR, Vaulot D (1999b) *Prochlorococcus*, a marine photosynthetic prokaryote of global significance. Microbiol Mol Biol Rev 63:106–127

Paytan A, Mackey KRM, Chen Y, Lima ID, Doney SC, Mahowald N, Labiosa R, Post AF (2009) Toxicity of atmospheric aerosols on marine phytoplankton. Proc Natl Acad Sci USA 106:4601–4605

Post AF (2005) Nutrient limitation of marine cyanobacteria—molecular ecology in an oligotrophic sea. In: Huisman J, Matthijs HCP, Visser PM (eds) Harmful cyanobacteria. Springer, Netherlands, pp 87–107

Richardson TL, Jackson GA (2007) Small phytoplankton and carbon export from the surface ocean. Science 315:838–840

Rivers AR, Jakuba RW, Webb EA (2009) Iron stress genes in marine *Synechococcus* and the development of a flow cytometric iron stress assay. Environ Microbiol 11:382–396

Rocap G, Larimer FW, Lamerdin J, Malfatti S, Chain P, Ahlgren NA, Arellano A, Coleman M, Hauser L, Hess WR, Johnson ZI, Land M, Lindell D, Post AF, Regala W, Shah M, Shaw SL, Steglich C, Sullivan MB, Ting CS, Tolonen A, Webb EA, Zinser ER, Chisholm SW (2003) Genome divergence in two *Prochlorococcus* ecotypes reflects oceanic niche differentiation. Nature 424:1042–1047

Scanlan DJ, Ostrowski M, Mazard S, Dufresne A, Garczarek L, Hess WR, Post AF, Hagemann M, Paulsen I, Partensky F (2009) Ecological genomics of marine picocyanobacteria. Microbiol Mol Biol Rev 73:249–299

Smith CJ, Osborn AM (2009) Advantages and limitations of quantitative PCR(Q-PCR)-based approaches in microbial ecology. FEMS Microbiol Ecol 67:6–20

Ting CS, Rocap G, King J, Chisholm SW (2002) Cyanobacterial photosynthesis in the oceans: the origins and significance of divergent light-harvesting strategies. Trends Microbiol 10:134–142

Waterbury JB, Watson SW, Guillard RRL, Brand LE (1979) Widespread occurrence of a unicellular, marine, planktonic, cyanobacterium. Nature 277:293–294

Webb EA, Moffett JW, Waterbury JB (2001) Iron stress in open-ocean cyanobacteria (*Synechococcus*, *Trichodesmium*, and *Crocosphaera* spp.): identification of the idiA protein. Appl Environ Microbiol 67:5444–5452

West NJ, Schonhuber WA, Fuller NJ, Amann RI, Rippka R, Post AF, Scanlan DJ (2001) Closely related *Prochlorococcus* genotypes show remarkably different depth distributions in two oceanic regions as revealed by in situ hybridization using 16S rRNA-targeted oligonucleotides. Microbiology 147:1731–1744

Wong GTF, Chao S-Y, Li Y-H, Shiah F-K (2000) The Kuroshio edge exchange process (KEEP) study—an introduction to hypotheses and highlights. Cont Shelf Res 20:335–347

Yuan W, Zhang J (2006) High correlations between Asian dust events and biological productivity in the western North Pacific. Geophys Res Lett 33:L07603

Zohary T, Herut B, Krom MD, Fauzi C, Mantoura R, Pitta P, Psarra S, Rassoulzadegan F, Stambler N, Tanaka T, Thingstad TF, Woodward EMS (2005) P-limited bacteria but N and P co-limited phytoplankton in the Eastern Mediterranean—a microcosm experiment. Deep Sea Res II 52:3011–3023

Zwirglmaier K, Heywood JL, Chamberlain K, Woodward EMS, Zubkov MV, Scanlan DJ (2007) Basin-scale distribution patterns of picocyanobacterial lineages in the Atlantic Ocean. Environ Microbiol 9:1278–1290

Zwirglmaier K, Jardillier L, Ostrowski M, Mazard S, Garczarek L, Vaulot D, Not F, Massana R, Ulloa O, Scanlan DJ (2008) Global phylogeography of marine *Synechococcus* and *Prochlorococcus* reveals a distinct partitioning of lineages among oceanic biomes. Environ Microbiol 10:147–161